Applied Soft Computing 51 (2017) 328–340

Contents lists available at ScienceDirect

Applied Soft Computing

journal homepage: www.elsevier.com/locate/asoc

Fusing feasible search space into PSO for multi-objective cascade reservoir optimization

Tao Bai[a,b], Yan-bin Kan[a], Jian-xia Chang[a], Qiang Huang[a], Fi-John Chang[b,*]

[a] State Key Laboratory Base of Eco-Hydraulic Engineering in Arid Area, Xi'an University of Technology, Jinhua Road 5, Xi'an, Shaan xi, China
[b] Department of Bioenvironmental Systems Engineering, National Taiwan University, No. 1, Sec. 4, Roosevelt Road, Da-An District, Taipei 10617, Taiwan, ROC

ARTICLE INFO

Article history:
Received 29 September 2015
Received in revised form 11 March 2016
Accepted 3 December 2016
Available online 7 December 2016

Keywords:
Multi-objective
Feasible search space-particle swarm optimization algorithm (FSS-PSO)
Optimal cascade reservoir operation
Water and sediment regulation

ABSTRACT

This study proposes a multi-objective optimization model of two cascade reservoirs in the Upper Yellow River basin for increasing social well-beings in general while simultaneously mitigating ice/flood threats. We first develop a strategy of dimensionality reduction and constraint transformation to largely diminish the complexity of the optimization system and next propose a novel search method that fuses a Feasible Search Space (FSS) into the Particle Swarm Optimization (PSO) algorithm, i.e. FSS-PSO, to effectively solve the optimization problem. To investigate the applicability and effectiveness of the proposed method, this study compares the FSS-PSO model with historical operation. The results indicate that the proposed model produces much better performances in all the objectives than historical operation. To assess the superiority and efficiency of the proposed FSS-PSO, the classical PSO and the Chaos Particle Swarm Optimization (CPSO) are also implemented to compare their computation time and convergence rates. The results demonstrate that the FSS-PSO improves the efficiency of the PSO and the CPSO by 72% and 55% accordingly and the convergence rate of the FSS-PSO is the fastest among the three algorithms. The results suggest that the proposed dimensionality-reduction strategy coupled with the FSS-PSO algorithm is a promising tool for water resources management under multi-objective joint reservoir operation and the proposed method could be easily implemented in the context of multi-objective optimization.

1. Introduction

The Yellow River is "China's Mother River" because its basin is the cradle of the Chinese civilization. The complex topography, fragile environment and prominent contradiction in various sectors make a considerable increase in flood and ice disasters over its upper basin, which threatens lives and property in downstream areas. As known, the Yellow River is famous for its sedimentation problems, where the suspended sediment has formed a secondary suspended river [25,28,32]. Reservoirs are the most effective water storage facilities in alleviating the uneven spatio-temporal distribution of water resources. As known, the purposes of most reservoirs built along the River in the past decades were only to generate hydropower in response to socio-economic development needs. With the rapid increase in water demand driven by population growth coupled with socio-economic development, the imbalances in water supply and demand, the tasks of flood and ice control and other factors have caused a dramatic change in the purposes of reservoir operation. Nonetheless, re-allocating the limited water resources of multi-purposed reservoirs is a great challenge, if not impossible.

System analysis is a very useful tool for assessing the impacts of policies and managing complex systems. Many engineering problems involve multiple competing objectives and prospective solutions. In the last decades, various classical nonlinear optimization methods have been used with effective and competent performance when tackling these problems. However, they usually require gradient information about the objective functions and constraints, which, in general, are difficult to solve and would easily fall into local optimal solutions. Recently, several meta-heuristic approaches, such as evolutionary algorithms (EA) [10,44], harmony search (HS) [18], biogeography-based optimization (BBO) [5] and particle swarm optimization (PSO) [42,45], have been proposed and utilized in order to handle diverse optimization tasks [4,17,19,30,31]. While these meta-heuristic methods produce better performances over classical optimization approaches in complex multi-objective problems, they are plagued by their own limitations such as premature convergence to a local optimal solu-

* Corresponding author.
E-mail address: changfj@ntu.edu.tw (F.-J. Chang).

http://dx.doi.org/10.1016/j.asoc.2016.12.005
1568-4946/

tion rather than a global on [35]. As known, in high dimensional problems, only a small percentage of solutions can converge to the entire Pareto optimal front, termed as the "curse of dimensionality" [16]. Deb and Saxena [14] indicated that the ability to fully explore surfaces in greater than five dimensions was highly limited. Consequently, more research efforts must be developed in this direction if many-objective problems are to be solved.

Various meta-heuristic approaches have revealed superior performance in dealing with complex hydrological operation systems [3,8,11,20,23,24,34,39]. Lately, swarm intelligence algorithms have become popular in solving reservoir planning and management problems, for example, the genetic algorithm (GA) [9,12,22,27,36,37]; artificial neural network (ANN) [6,13]; ant colony optimization (ACO) [1]; and the PSO [2,7,21,26,36]. Even through efficient swarm intelligence algorithms satisfactorily applied to many optimization problems, the PSO algorithm, however, has its own flaws, e.g. early maturity, slow convergence rates, or difficult to handle constraint optimization problems. For this reason, a number of studies have been proposed to improve the efficiency and/or effectiveness of the PSO algorithm through adjusting its code mode, inertia weight, maximum speed limit of particles, mutation operators, neighborhood operations, boundary conditions [15,29,33,44]. Some of the studies used hybrid (mixture and parallel) algorithms, for instance PSO with immune algorithms, simulated annealing algorithms and chaos algorithms, to improve search effectiveness [38,40,41].

In this study we aim to find a suitable water and sediment regulation strategy for multi-objective reservoir operation through searching a set of optimal solutions for two pivotal cascade reservoirs in the Upper Yellow River basin. We propose a dimensionality-reduction and constraint transformation procedure coupled with a novel search strategy that fuses a Feasible Search Space (FSS) into the PSO algorithm, i.e. an improved PSO algorithm (FSS-PSO), to effectively search optimal solutions. Our research findings would suggest optimal operation strategies for water and sediment conservation and provide the referential impacts of water allocation on sediment control. The rest of the present article is structured as follows: Section 2 is dedicated to the mathematical representation of cascade reservoirs with the explanation of the implementation procedure of the proposed FSS-PSO algorithm; Section 3 explains the study watershed and model construction; Section 4 presents and discusses the experimental results, comparison and evaluation of the performance of the investigative methods. Finally, the conclusion of the implementation of the proposed method is presented in the last Section.

2. Methods

Water resources management often involves very large scale measures, complex processes and regulations. It is a great challenge to make efficient water resources management that optimizes a real-practical system under the great uncertainty of hydro-meteorological conditions. We propose a multi-objective optimization model for the joint operation of two cascade reservoirs in the Upper Yellow River basin for decision makers to increase social well-beings while simultaneously mitigate ice/flood threats. We first derive a mathematical model that considers four objectives: water and sediment regulation; ice and flood control; power generation; and water supply, and then provide a clear perspective of all the consideration and physical constraints conditions. To solve the complex problem, a dimensionality-reduction and constraint transformation procedure is proposed while a novel and effective search method, i.e. FSS-PSO, is developed and evaluated. The core idea of the FSS-PSO is to intelligently handle the objectives and constraints through intelligibly refining the feasible search space. To assess the proposed FSS-PSO, the classical PSO and the chaos particle swarm optimization (CPSO) are also implemented to compare the computation time and convergence rates of the three algorithms. The research flowchart of this study is illustrated in Fig. 1. A detailed description of the methods adopted in this study is shown as follows.

2.1. Building a multi-objective model and its transformation

The multi-objective optimization problem can generally be expressed as follows.

$$\text{Minimize/Maximize} F(X) = [F_1(X), F_2(X), .., F_k(X)] \tag{1}$$

$$\text{subject to} G_i(X) \leq 0, i = 1, 2, .., m.$$

$$H_j(X) = 0, j = 1, 2, .., p,$$

where $F(X)$ is a vector of objective functions; G_i (X) and H_j (X) are constraints; k is the number of objective functions; m is the number of inequality constraints; and p is the number of equality constraints. X is a vector of decision variables.

A common solution for multi-objective optimization problems is to determine a Pareto optimal set. However, the difficulty in finding a representative Pareto front set would arise significantly as the dimension increases. To solve the problem, we propose to reduce the number of objectives and to identify any constraint that actually restrains the FSS for the stated objectives. The mathematical expression of objectives and constraints of an optimization model can be generally classified into two types: equality and inequality. The inequality objectives must be strictly satisfied in the search process, and thus they could be transformed into strong constraints. As a result, the number of objectives of the multi-objective optimization model could be reduced, which would decrease the dimension as well as the difficulty in searching the optimal solution.

The controllable variables for reservoir operation can be classified into three categories: discharge; water level; and power generation. We, thus, classify the constraints into the three categories based on their features. These constraints are further divided into two types: transformable constraint; and non-transformable constraint. Transformable constraints can be directly converted into decision variables while non-transformable constraints are, in general, the implicit functions of optimization variables, which cannot be converted into decision variables. The category of controllable variables and the classification of constraints are listed in Table 1 .

2.2. Refining feasible search space (FSS)

In this study, the non-transformable constraints (i.e. power generation output) can be decomposed into E_1 and E_2, in which E_1 is a composite function addressing the composition of relations between water head and generated flow while E_2 is a composite function in relation to the power generation output of different power generating units. The targets of E_1 and E_2 are to make the maximum generation benefit in a dispatch period. The concept of refining the FSS is presented in Fig. 2, and the relevant process is addressed as follows.

2.2.1. Process description

First of all, the whole dispatch period $[0, T]$ is equally divided into T intervals. In our case, the whole dispatch period is one year and the intervals are of a monthly scale. The FSS can then be refined (filtered) sequentially by cross-examining the objectives and transformable constraints in the pairs of consecutive sub-periods. The process of refining the FSS of the whole dispatch period begins with

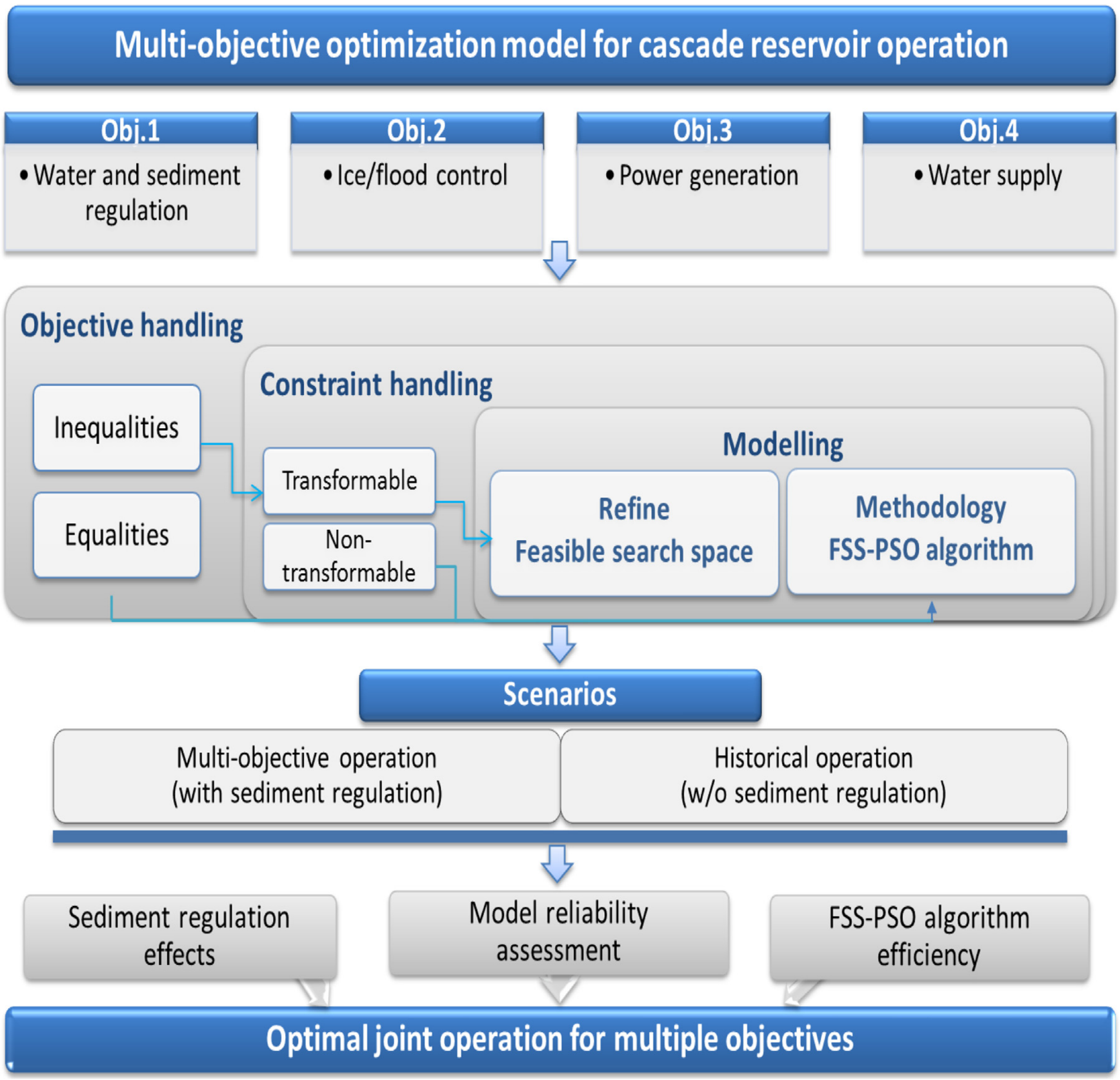

Fig. 1. Research flowchart.

Table 1
Constraint classification.

Transformable		Non-transformable
Discharge/outflow - flow for water supply - ecological flow - flow for flood control	Water level - water balance - reservoir storage capacity - water level • dead water level • dead water level • water level for flood control	Power generation - installed capacity - guaranteed output of power generation

the pair of consecutive sub-periods: [0, T-1] and [T-1, T], then the similar refining process is repeatedly applied to the pairs of [0, T-2] & [T-2, T-1], . . ., and [0, 1] & [1, 2]. Therefore a total of T-1 refining processes are sequentially implemented, in which the FSS is backwardly refined from [T-1, T] to [0, 1]. The steps of the refining process implemented from [0, T] to [0, 1] are described in details, shown as follows.

Step 1: Period [0, T]. The period [0, T] is divided into a pair of sub-periods [0, T-1] and [T-1, T]. The water levels of reservoir i at the beginning (t = 0) and the end (t = T) are assigned the same value, i.e. $Z(i, 0) = Z(i, T)$. In each sub-period, the water level should fall within the range of the final water level of its corresponding sub-period.

(1) For [0, T-1], the range of water level is denoted as Z_0, shown as follows.

$$Z_0(i, T-1) \in [Z^0_{\min}(i, T-1), Z^0_{\max}(i, T-1)] \tag{2}$$

Given the initial water level$Z(i, 0)$, the range of the final water level is thus narrowed from $[Z^0_{\min}(i, 0), Z^0_{\max}(i, 0)]$ to $[Z^0_{\min}(i, T-1), Z^0_{\max}(i, T-1)]$ (Fig. 2).

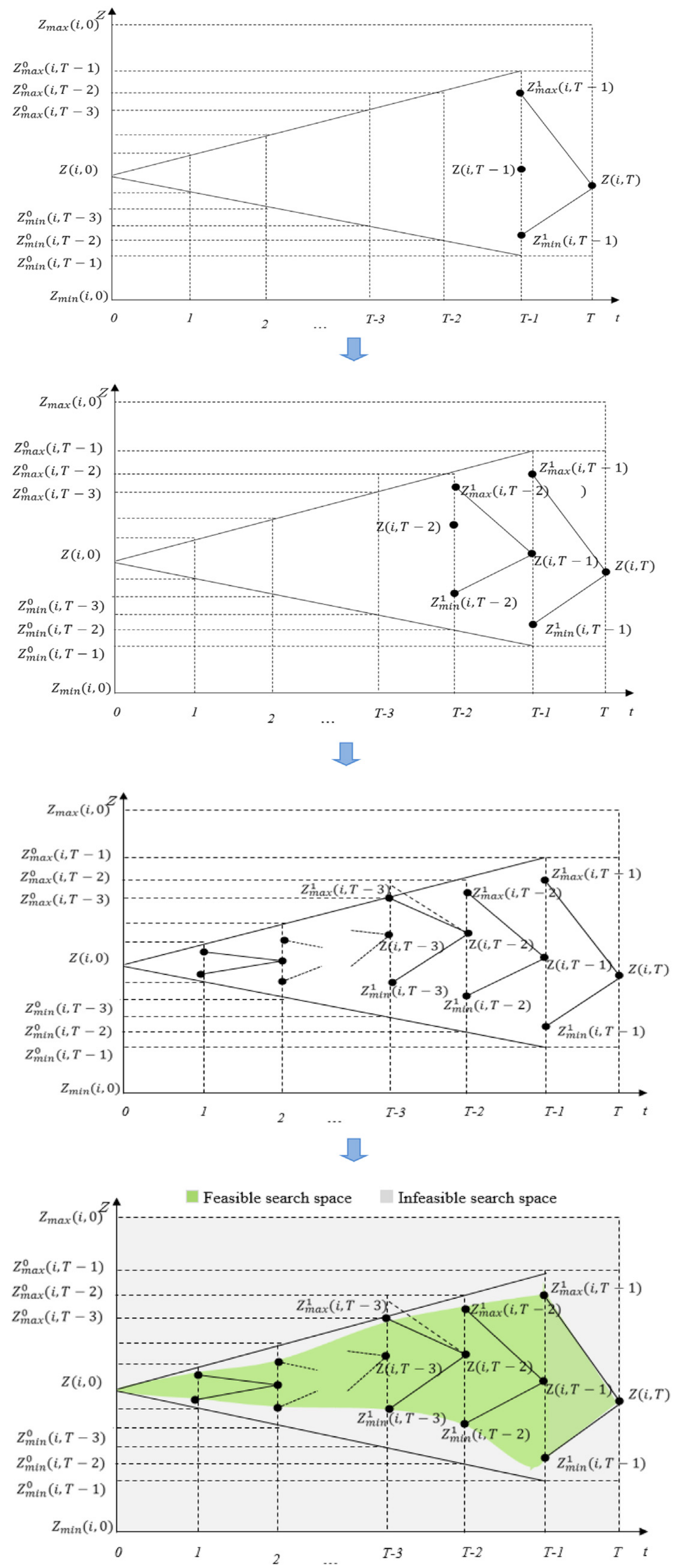

Fig. 2. Refinement of the feasible search space.

(2) For 〔T-1, T〕, the final water level$Z(i, T)$is set the same as the initial water level $Z(i, 0)$. Based on transformable constraints, the range of the initial water level, denoted as Z_1, is spanned and expressed as follows.

$$Z_1(i, T-1) \in [Z^1_{\min}(i, T-1), Z^1_{\max}(i, T-1)] \tag{3}$$

Therefore, the range of the initial water level is narrowed from $[Z^0_{\min}(i, T-1, Z^0_{\max}(i, T-1)]$ to $[Z^1_{\min}(i, T-1), Z^1_{\max}(i, T-1)]$ (Fig. 2).

(3) Combining the results of the previous sub-steps (1) and (2), the intersection of the final water level of 〔0, T-1〕 and the initial water level of 〔T-1, T〕 confines the water level at T-1, which falls within $[Z^1_{\min}(i, T-1), Z^1_{\max}(i, T-1)]$ (Fig. 2).

Step 2: Period 0, 〔T-1〕. In the same way, the second period 〔0, T-1〕 is divided into a pair of consecutive sub-periods 〔0, T-2〕 and 〔T-2, T-1〕.

(1) For 〔0, T-2〕, the water level of reservoir i begins with$Z(i, 0)$and the final water level can be obtained in the same way shown in *Step 1*. Thus the range of the final water level is narrowed from $[Z^0_{\min}(i, T-1), Z^0_{\max}(i, T-1)]$to $[Z^0_{\min}(i, T-2), Z^0_{\max}(i, T-2)]$.
(2) For 〔T-2, T-1〕, the final water level at T-1 is generated by a stochastic approach within $[Z^1_{\min}(i, T-1), Z^1_{\max}(i, T-1)]$ (Fig. 2). Then the range of the initial water level that meets all constraints can be obtained, denoted as $[Z^1_{\min}(i, T-2), Z^1_{\max}(i, T-2)]$.
(3) By taking the intersection of $[Z^0_{\min}(i, T-2), Z^0_{\max}(i, T-2)]$, i.e. the final water level of〔0, T-2〕, and $[Z^1_{\min}(i, T-2), Z^1_{\max}(i, T-2)]$, i.e. the initial water level of 〔T-2, T-1〕, the range of water level at T-2 is narrowed from $[Z^0_{\min}(i, T-2), Z^0_{\max}(i, T-2)]$ to$[Z^1_{\min}(i, T-2), Z^1_{\max}(i, T-2)]$.

2.2.1.1. Step 3: Repeat the refining process. The refining process is repeatedly conducted for the periods of〔0, T-2〕,〔0, T-3〕,. . ., and〔0, 2〕. It is noticed that the intersection may exceed the boundary spanned by the initial water level$Z(i, 0)$, as shown at $T-3$of the third period 〔0, T-2〕. Therefore, its range is confined to $[Z^1_{\min}(i, T-3), Z^0_{\max}(i, T-3)]$over 〔0, T-2〕.

2.2.1.2. Step 4: Confine the FSS for the whole dispatch period. The range of water level for reservoir i over the whole dispatch period 〔0, T〕 can be obtained from the refining processes. The final step is to individually link the maximum and minimum water levels of T intervals for confining the FSS over the whole dispatch period〔0, T〕, i.e. the green area shown in Fig. 2 is the desired FSS.

In brief, the original search space of the model spans over $[Z_{\min}(i, 0), Z_{\max}(i, 0)]$in the whole dispatch period〔0, T〕. (Fig. 2) The refining process systematically excludes infeasible solutions that do not satisfy transformable constraints. Most importantly, the search space can be effectively confined to the FSS through the refining process. Consequently, the FSS for the PSO can be identified, which greatly enhances the efficiency and accuracy of the algorithm.

2.3. Implementation steps of the FSS-PSO

The implementation flowchart of the FSS-PSO is shown in Fig. 3, and the main procedures are addressed as follows.

2.3.1. Step 1: Parameter setting

In this study, the cascade reservoirs are denoted as $i(i=1$, or 2) and the dispatch period is $T(T=12$ months). The water level is selected as the particle position in the PSO. Then the position of the *ith*particle in the T-dimensional search space is $Z(i, T)$. The population size of the particle is m, and the iteration number is k. The basic parameters consist of: learning factors c_1, c_2; the minimum and maximum weight coefficients $w_{\min}, w_{\max}$, which are random numbers between 0 and 1; the maximum velocity $v_{\max}$; the penalty coefficient σ; and the stopping criterion ε_0, i.e. precision demand. Parameters of the FSS-PSO are determined mainly according to our previous experiences: (1) population size is determined by the numbers of objective functions, constraints and decision variables; (2) the number of iterations is determined by the convergence speed; (3) learning factors c_1, c_2, $w_{\min}$, $w_{\max}$, $v_{\max}$and penalty coefficient σ are determined by an overall assessment of the three investigative algorithms (FSS-PSO, CPSO, PSO); and (4) stop criteria ε_0 is determined by the attributes and accuracy of the decision variables.

2.3.2. Step 2: Constraints handling

Based on the known initial and final water levels of each reservoir, the initial sequence$Z(i, 1)$, …,$Z(i, T-1)$,$Z(i, T)$can be randomly assigned within the FSS refined previously, which satisfies all the transformable constraints.

2.3.3. Step 3: Initialization of the PSO

The initial position and velocity of the PSO are initialized within the FSS, and each particle is classified into the elite set and considered as an individual extremumP_i.

2.3.4. Step 4: Selection and calculation of fitness values

Take the objective function as the fitness for each particle. Then the fitness value of each particle can be calculated before the iteration begins.

2.3.5. Step 5: Update of the position and velocity for each particle

A global extremum P_g can be selected from the elite set by roulette wheel selection. Then the position and velocity of each particle in the elite set are updated according to the update formulas of position and velocity in the PSO ([26]).

2.3.6. Step 6: Constraint checking

Check whether the updated particle satisfies all the non-transformable constraints or not. If not, the updated particle will be abandoned from the elite set and new particle will be generated through particle swarm initialization.

2.3.7. Step 7: Calculation of the fitness value for the new particle to compare and select a better particle

When the number of particles in the elite set exceeds the population size, particles with smaller fitness values would be excluded from the elite set. If the current position of a particle is superior to the individual extremumP_i, then replaceP_i. Otherwise, keep the individual extremum P_i and update the positions and velocities of five percent of particles through re-initialization.

2.3.8. Step 8: Stop criterion checking

Check whether the iteration termination condition is reached or not. Either the current iteration number reaches the preset iteration number or the fitness value of the particle reaches the minimum requirement, the iteration stops and the optimization results are delivered. Otherwise, go to *Step 5*.

Finally, the FSS-PSO identifies the elite set that can be considered as the global equilibrium solution set of the multi-objective optimization model.

3. Study watershed and model construction

In this study, the Ningxia-Inner Mongolia reaches (hereinafter referred to as the Reaches) are selected as the control objects. Being

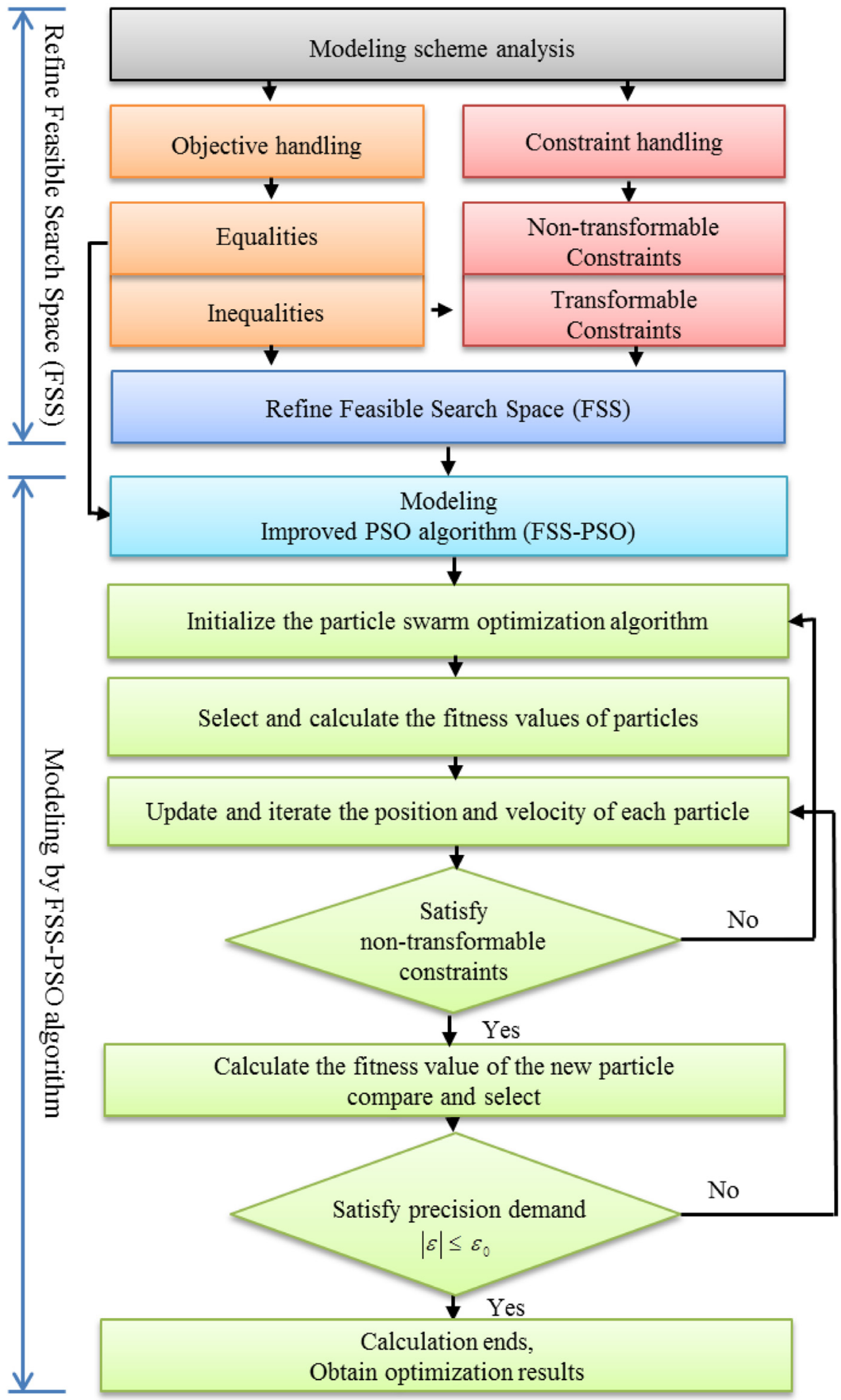

Fig. 3. Implementation steps of Refine Feasible Search Space (a) and the improved PSO (FSS-PSO).

located at the northernmost region of the Yellow River basin, the Reaches extend 1080 km from Xiaheyan (*XHY*), Zhongwei City of Ningxia Province to Toudaoguai (*TDG*), Tuoketuo County of Inner Mongolia Province, over which six main hydrologic stations are situated (Fig. 4). In this study, artificial floods are produced by the cascade reservoirs of *LYX* and *LJX*, which are situated in the Upper Reaches for maintaining the comprehensive utilization of hydropower generation, water supply, and flood and ice control. The watershed of the *LYX* reservoir occupies an area of 0.13 million km^2, and the effective storage capacity of the reservoir reaches 19.35 billion m^3, which makes the *LYX* the only reservoir equipped with multi-year water regulation ability along the Yellow River. The normal water level, water level for flood control and dead water level of the *LYX* reservoir are 2600m, 2594 m and 2530m, respectively. As for the *LJX* reservoir, its watershed occupies an area of 0.18

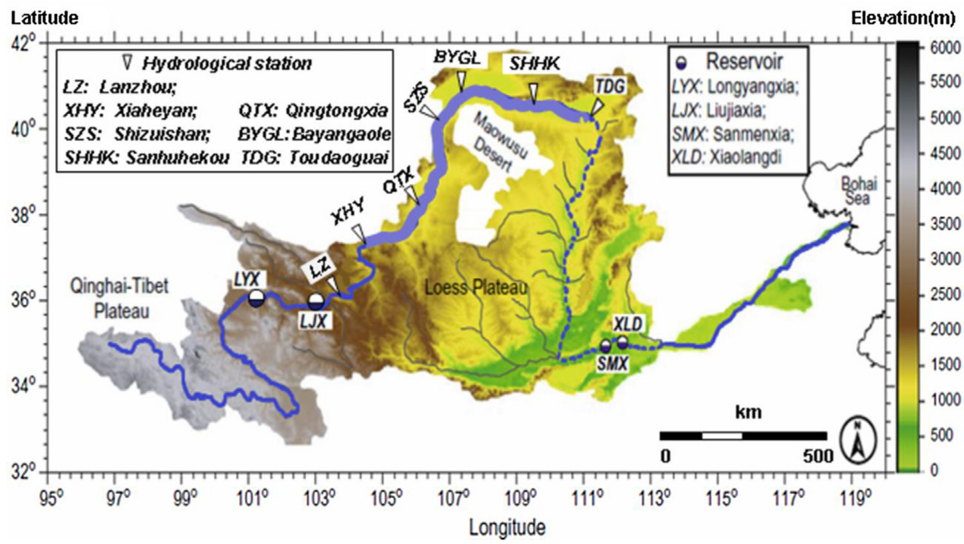

Fig. 4. Map of the Yellow River basin, including the locations of major hydrological stations and reservoirs. The dotted line represents the Middle Yellow River that partitions the Yellow River into the Upper Yellow River (upper TDG station) and the Lower Yellow River. The thick blue line represents the Ningxia-Inner Mongolia reaches in the Upper Yellow River basin.

million km^2 while its effective storage capacity is 5.7 billion m^3, and thus the *LJX* reservoir implements water regulation annually.

3.1. Materials

There are six main hydrological stations in the Reaches while the Lanzhou (*LZ*) station, another station controlling the water supply of the whole Yellow River, is located in the Upper Yellow River basin. Moreover, the average flow and sediment data at each hydrological station during the flood periods of the past 60 years (1953–2013) are used to analyze the relationship between water and sediment for obtaining reasonable and effective flushing flow in consideration of sediment regulation. The investigative data consist of the monthly data collected from the reservoirs, the river channels, the tributaries and irrigation districts and ice and flood control conditions.

3.2. Model construction

3.2.1. Objective and constraints

The model considers four objectives (water and sediment regulation, power generation, ice/flood control and water supply) and five types of constraints (water balance, water balance between reservoirs, water level, outflow and power generation output), which are addressed as follows.

3.2.1.1. Objective 1 (Obj.1): Water and sediment regulation.

$$\max W = \max(\sum_{n=1}^{N}\sum_{t=1}^{T} w(n,t)\cdot \Delta t) \tag{4}$$

$$w(n,t) = K \cdot Q^a(n,t)\cdot S^b(n,t) \tag{5}$$

where $W$is the sediment discharge of the whole Reaches; $w(n, t)$is the sediment transport rate of section n at time t; N is the number of sediment transport sections; $Q(n, t)$ is the sediment discharge at outlet section n at time t; $S(n, t)$is the sediment concentration of section n at time t; and K, a, $b$are parameters determined by the relationship of discharge and sediment at six sections.

3.2.2. Objective 2 (Obj.2): Ice/flood control

The main channel of the Reaches would freeze during the end of November and the next March (ice control period). The *LJX* reservoir is a regulation reservoir, and its discharge is controlled by the Yellow River Conservancy Commission (YRCC) for making sure the safety of downstream areas. The objective of ice control is to minimize the maximum absolute difference between the actual outflow and the controlled flow of the reservoir, described as follows.

$$\min(\max|Q(Liu,t) - Q_o(t)|) \tag{6}$$

where $Q(Liu, t)$is the outflow of the *LJX* reservoir; and $Q_o(t)$ is the threshold of outflow, which meets the ice control requirement given by the YRCC.

To ensure the safety of dams and downstream areas in flood periods the water level and outflow of each reservoir must be controlled within certain ranges, shown as follows.

$$Z_{\min}(i,t) \le Z(i,t) \le Z_{\max}(i,t) \tag{7}$$

$$Q_{o\min}(i,t) \le Q(i,t) \le Q_{o\max}(i,t) \tag{8}$$

where $Z(i, t)$and $Q(i, t)$ are the water level and outflow of the *ith* reservoir at time t, respectively; and $Z_{\min}(i, t)$and $Z_{\max}(i, t)$ are the minimum and maximum allowable water levels of the *ith* reservoir at time t, respectively. $Z_{\min}(i, t)$ is the dead water level; $Z_{\max}(i, t)$ is the water level for flood control. $Q_{o\min}(i, t)$ and $Q_{o\max}(i, t)$ are the minimum and maximum allowable outflow, respectively.

3.2.3. Objective 3 (Obj.3): Hydropower generation

Hydropower generation is one of the most important objectives for the two reservoirs, which is defined as follows.

$$E = \max\sum_{i=1}^{M}\sum_{t=1}^{T} N(i,t)\times\Delta t \qquad \forall i \in M, t \in T \tag{9}$$

where E is the total power generation output in a given operation period; $N(i, t)$ is the power generation output of the *ith* hydropower station at time t; Δt is the duration; M is the number of hydropower stations; and T is the operation period.

3.2.4. Objective 4 (Obj.4): Water supply

According to the Integrated Planning of Water Resources on the Yellow River, published by the YRCC, the flow of the *LZ* section is selected to satisfy the water supply demand of the whole watershed, shown as follows.

$$Q\,(Lanzhou, t) \geq Q\min(t) \tag{10}$$

where $Q\,(Lanzhou, t)$ is the flow in the *LZ* section at time t; and$Q\min(t)$ is the minimum flow in the *LZ* section required for maintaining the balance between supply and demand of water resources.

Constraints of the multi-objective optimization model are addressed below.

(1) Water balance

$$Q(i, t) = Q(i-1, t) + [Q_I(i, t) - Q_W(i, t) - Q_L(i, t) + Q_B(i, t)] \tag{11}$$

where $Q(i, t)$ is the flow of the *ith* reservoir at time t;$Q_I\,(i, t)$,$Q_W\,(i, t)$, $Q_L\,(i, t)$and$Q_B\,(i, t)$ are the interval inflow, water supply flow, lost flow, and backwater flow from irrigation areas between the $i-1th$ reservoir and the *ith* reservoir at time t, respectively; and $Q(i-1, t)$ is the flow of the $i-1th$ reservoir at time t.

(2) Water balance between reservoirs

$$V\,(i, t+1) = V\,(i, t) + (Q_I\,(i, t) - Q_O\,(i, t)) \times \Delta T\,(t) \tag{12}$$

where $V\,(i, t+1)$ and $V\,(i, t)$ are the initial storages of the *ith* reservoir at times $t+1$ and t, respectively; $Q_I\,(i, t)$ and$Q_O\,(i, t)$ are the inflow and outflow of the *ith* reservoir, respectively; and $\Delta T\,(t)$ is the duration.

(3) Water level

$$Z_{\min}(i, t) \leq Z(i, t) \leq Z_{\max}(i, t) \tag{13}$$

where $Z_{\min}(i, t)$ and $Z_{\max}(i, t)$ are the dead water level and the maximum water level of the *ith* reservoir, respectively.

(4) Outflow

$$Q_{O\min}(i, t) \leq Q_O(i, t) \leq Q_{O\max}(i, t) \tag{14}$$

where $Q_{O\min}(i, t)$and$Q_{O\max}(i, t)$ are the minimum and maximum allowable outflow of the *ith* reservoir at time t, respectively.

(5) Power generation output

$$N_{\min}(i, t) \leq N(i, t) \leq N_{\max}(i, t) \tag{15}$$

where $N\,(i, t)$, $N_{\min}\,(i, t)$and$N_{\max}\,(n, t)$ are the power generation output, minimum output and maximum output of the *ith* reservoir at time t, respectively. In general, $N_{\min}\,(i, t)$is the guaranteed output of power generating units and $N_{\max}\,(i, t)$ is the installed capacity.

The importance and regulation of each objective in various periods, however, could be very different. For example, the other objectives must make a concession to the safety requirements of ice control during ice control periods, that is to say, the flow in the *LZ* section and the discharge of the *LJX* reservoir must be controlled subject to the flow requirements for ice control. Details of the priority of objectives considered in various periods are shown in Table 2.

3.2.5. Search methods

The established model would be solved by the FSS-PSO algorithm. The first step is objective handling. The objectives of water supply and flood/ice control are given in the form of inequality, which are transformed into strong constraints. On the other hand, the objectives of hydropower generation and water and sediment regulation are revised and expressed as follows.

$$B = \max f(\lambda_1 E(i, t), \lambda_2 W(n, t)) = \max f(\lambda_1 \sum_{i=1}^{\mathrm{M}} \sum_{t=1}^{T} N(i, t) \cdot \Delta t, \lambda_2 \sum_{n=1}^{\mathrm{N}} \sum_{t=1}^{T} w(n, t) \cdot \Delta t)) \tag{16}$$

where $B$is the global equilibrium solution of the objective function; and $E(i, t)$, $W(n, t)$ are the sub-objective functions of reservoir i at time t and section n at time t, respectively. $\lambda_1$and$\lambda_2$are the weight coefficients of the corresponding sub-objectives.

The next step is to classify constraints into transformable and non-transformable constraints so that the FSS can be refined, as shown in Fig. 2. The details of the constraints and parameters of the FSS-PSO are listed in Tables 3 and 4, respectively.

In this study, there are a number of major settings that need to be assigned before modelling: (1) the water level of the *LJX* reservoir must decrease to 1726 m at the start of flood periods while to 1728 m at the start of ice control periods to make sure that the reservoir has enough capacity for flood/ice control operation; (2) the water level of the LYX reservoir must decrease to 2594 m at the start of flood periods; (3) the flow of the *LZ* section and the outflow of the *LJX* reservoir must satisfy the minimum flow requirement of the *LZ* section; (4) the outflow of the *LJX* reservoir must comply with the Ice Flood Control Plan of the Yellow River to ensure the ice/flood safety of the whole watershed; (5) the minimum flow required for the water and sediment regulation in the Sanhuhekou (*SHHK*) section exceeds 2580 m^3/s, which is obtained from the average flow and sediment data of the flood periods in the past 60 years (1953–2013); and (6) the guaranteed outputs of the *LYX* and *LJX* hydropower stations are 600 MW and 400MW, respectively, while the installed capacities of the *LYX* and *LJX* hydropower stations are 1280 MW (maximum discharge: 1200 m^3/s) and 1350 MW (maximum discharge: 1552 m^3/s), respectively. In particular, hydropower generation should come to a compromise with the safety requirements of dams and downstream areas in ice control periods.

4. Results and discussion

4.1. Regulation timing

In general, the operations of water and sediment regulation can only be carried out in wet years so that there will be enough water to ensure a smooth implementation of water and sediment regulation. The reservoir operation in 2010 is selected as a case study because year 2010 was a wet year and the water level of the *LYX* reservoir was high. Based on the operational experiences of the Xiaolangdi (*XLD*) reservoir, the adequate time for the *XLD* reservoir to implement water and sediment regulation is in the end of June [28]. However, the water and sediment regulation in the Reaches is conducted in March and April for two reasons: (1) to make a good connection with the water and sediment regulation of the *XLD* reservoir; and (2) the travel time of a flood from the Upper Yellow River to the *XLD* reservoir may take about 1–2 months. In this study, the dispatch period for water and sediment regulation will be lasted for 30 days (from 1st to 30th of April) to enhance the effectiveness of water regulation on the amount of sediment transport in the river channel.

Table 2
Implementation priority of objectives in various periods for the multi-objective optimization model.

Operation period (Month)	Objective implementation priority	
	LYX	LJX
Ice control period (11, 12,1,2,3)	Obj.2 > Obj.3 > Obj.4	Obj.2 > Obj.4 > Obj.3
Water supply period (4, 5)	Obj.4 > Obj.3 > Obj.1	Obj.4 > Obj.1 > Obj.3
Power generation period (6)	Obj.3 > Obj.4 > Obj.2	Obj.3 > Obj.4 > Obj.2
Flood control period (7, 8)	Obj.2 > Obj.3 > Obj.1	Obj.2 > Obj.1 > Obj.3
Power generation period (9, 10)	Obj.3 > Obj.2 > Obj.1	Obj.3 > Obj.2 > Obj.1

Table 3
Constraints of the FSS-PSO model.

Reservoir		LYX			LJK		
Constraints		Water level (m)	Discharge (m^3/s)	Output (10^4 kW)	Water level (m)	Discharge (m^3/s)	Output (10^4 kW)
Ice season	Max	2594	1200	128	1728	740,490,460,380,450	122.5
(Nov.-next March)	Min	2530	552	60	1694	740,490,460,380,450	40
Water & sediment	Max	2600	2698	128	1735	2820	122.5
(April)	Min	2580	2358	60	1728	2480	40
Water supply	Max	2600	1200	128	1735	1552	122.5
(May)	Min	2560	552	60	1694	1100	40
Flood season	Max	2594	4500	128	1726	1552	122.5
(July, Aug.)	Min	2530	650	60	1694	800,750	40
Others	Max	2600	1200	128	1735	1552	122.5
(June, Sep, Oct.)	Min	2530	552	60	1694	900,750,800	40

Table 4
Parameters of the FSS-PSO model.

Parameters	Value	Parameters	Value
Number of objective functions	2	Minimum weight coefficient (w_{min})	0.9
Number of constraints	24	Maximum weight coefficient (w_{max})	0.4
Number of decision variables	24	Maximum velocity coefficient (v_{max})	0.1
Population size (m)	500	Penalty coefficient (σ)	10^5
Number of iterations (k)	500	Stopping criterion in iteration (ε_0)	0.01
Learning factors (c_1, c_2)	2.0		

4.2. Scenario setting and initial condition

To assess model performance, the proposed FSS-PSO search method with water and sediment regulation as an objective is compared with historical operation that did not consider water and sediment regulation. According to the measured data collected from the historical operation in 2010, the initial conditions for the proposed FSS-PSO method during the period of January and December in 2010 are set as follows: the water level of the *LYX* is 2584.14m; the water level of the *LJX* is 1733.44m; and the discharge of the *LJX* during the period of water and sediment regulation is 2698 m^3/s, which is estimated by the interval runoff and the regulated flow of each section.

4.3. Performance analysis

4.3.1. Water and sediment (Obj.1)

According to the discharge of the *LJX* and the inflow from tributaries in each section of the Reaches, the flow of the sections where six hydrological stations are located can be calculated. Based on the observational data of sediment concentration, the relationship between sediment transport rate, section flow and sediment concentration of the upstream stations could be established ([43]). Take the *TDG* section as an example (Fig. 5), the performance of water and sediment regulation implemented by the optimal joint operation of cascade reservoirs is shown in Table 5.

As shown in Fig. 6, an artificial flood for water and sediment regulation is produced and the outflow of the *LJX* reservoir is 2680 m^3/s, which satisfies the flow constraint of water and sediment regulation. Based on the flow requirements of the water balance between intervals, the incoming and diverted water in each interval is considered and the flows in the seven sections between the *LZ* section and the *TDG* section are 2820m^3/s, 2730m^3/s, 2510m^3/s, 2650m^3/s, 2467m^3/s, 2580m^3/s and 2570m^3/s, respectively. For the artificial flood produced by the *LYX* and the *LJX* reservoirs, the sediment discharge of flood events ([43]) is used to construct the relationship of flow and sediment quantitatively. Then, the transported sediment volumes in each section are calculated, as shown in Table 5 wherein sediment concentrations and incoming sediment are the measured data collected in 2010. Based on the balance principle of sediment discharges between six sections, the scour and deposition in the five intervals are listed in Table 5, which also shows the scour condition or silt status of each interval.

Besides, the transported sediment exceeds the incoming sediment in each of the last four intervals. Almost all the riverbed of the Reaches is scoured by the artificial flood, and the total amount of scoured sediment exceeds 38.51 million tons, which can be reflected from the summation of the items in the row of "scour and deposition in an interval" in Table 5. In spite of the serious silted condition in the past, all the intervals are scoured except for the little silt of the interval *XHY-QTX*. As a result, more than 61.1 million tons of sediment is transported from the *TDG* section into downstream, which demonstrates a great improvement of the serious silt condition in the Reaches could be made through the water and sediment regulation suggested by the FSS-PSO model.

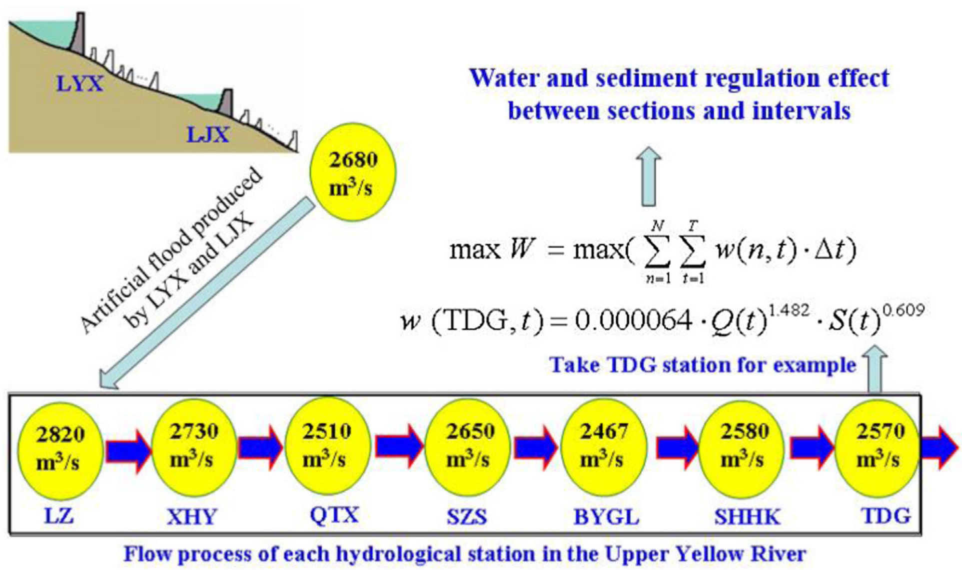

Fig. 5. Conversion of flow and sediment transported in each section and each interval for 2010.

Table 5
Performance of water and sediment regulation for 2010.

Item	Section					
	XHY	QTX	SZS	BYGL	SHHK	TDG
Flow (m^3/s)	2730	2510	2650	2467	2580	2570
Sediment concentration (kg/m^3)	4.430	4.280	4.340	4.920	6.960	8.340
I: Incoming sediment (10^8t)	0.3050	0.2440	0.2950	0.3110	0.4770	0.5810
T: Transported sediment (10^8t)	0.2269	0.2466	0.3503	0.3324	0.4479	0.6110

Item	Interval				
	XHY-QTX	QTX-SZS	SZS-BYGL	BYGL-SHHK	SHHK-TDG
S: Sediment in an interval (10^8t)	−0.0023[a]	0.0023	−0.0221	0.0042	−0.0110
Scour and deposition in an interval (10^8t) ($=I_n - T_{n+1} + S_n$)	0.0561	−0.1040	−0.0595	−0.1327	−0.1450

[a] A negative value of sediment indicates a scour condition, otherwise a silt status.

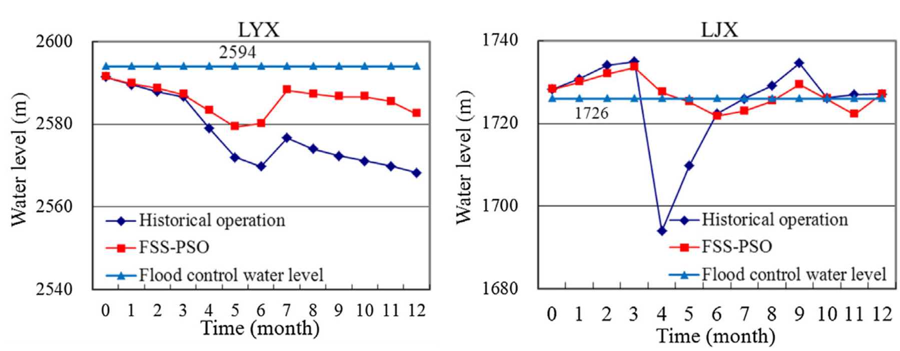

Fig. 6. Monthly water levels of the LYX and LJX reservoirs obtained from the FSS-PSO and historical operation for 2010, respectively.

4.3.2. Ice/flood control (Obj.2)

Fig. 6 shows that the water levels of the *LYX* and the *LJX* in flood seasons (mainly during July-August) obtained from the FSS-PSO model and historical operation. Results indicate that the water levels of the FSS-PSO are lower than the water levels required for flood control, i.e. 2594 m for the *LYX* and 1726 m for the *LJX*, respectively (flood control requirement).

Fig. 7 shows that the discharge of the *LJX* reservoir is lower than the control flow value requested by the Ice Flood Control Plans (released in 2009–2010 and 2010–2011), which describe the safety requirements of dams and downstream areas during ice control periods (Nov-next March). Furthermore, the discharge of the *LJX* of the FSS-PSO model is lower than that of historical operation during ice seasons, which demonstrates the FSS-PSO performs better than historical operation.

4.3.3. Power generation (Obj.3)

Fig. 8 shows that the outputs of the FSS-PSO model are, in general, much higher than the guaranteed output of the *LYX* and the *LJX* reservoirs, which meet the demand of power generation output. Such condition does not hold in ice seasons because a concession to the safety requirements of ice control must be made.

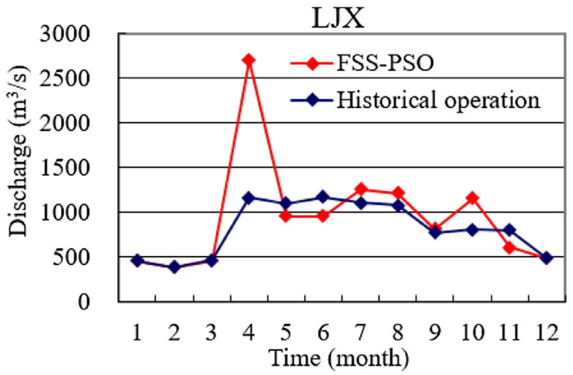

Fig. 7. Discharge of the LJX reservoir obtained from the FSS-PSO model and historical operation in 2010.

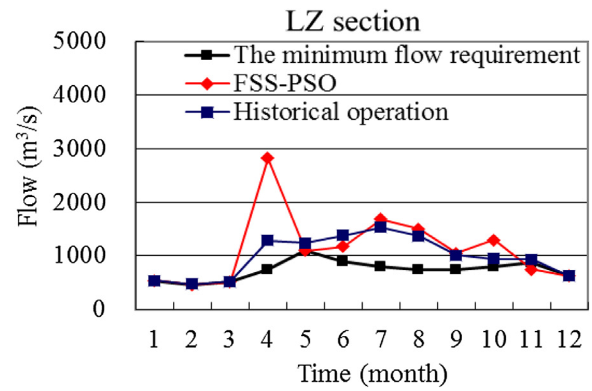

Fig. 9. Flow of the LZ section obtained from the FSS-PSO results and historical operation, respectively, for 2010.

4.3.4. Water supply (Obj.4)

Fig. 9 shows that the flow of the *LZ* section obtained from the FSS-PSO model is higher than the minimum flow requirement listed in Table 2, which meets the water supply demand, except for ice/flood seasons. We notice that the water supply of the *LZ* section does not fully satisfy the water demand in ice/flood seasons due to the safety requirements of ice/flood control.

In sum, the results nicely demonstrate that: (1) in consideration of the safety requirements of ice/flood control and the assurance of water supply and power generation demands, artificial floods are produced by the joint operation of cascade reservoirs and the produced large flow will last for one month, i.e. 1st – 30th of April; (2) the riverbed between the *QTX* and the *TDG*, i.e. the whole Reaches, is scoured by artificial floods, and the total amount of sediment scoured reaches 38.51 million tons (Table 5); and (3) compared with the historical data of the TDG, more than 61.10 million tons of sediment are transported, which is 4–5 times higher than historical data of water and sediment regulation for the same period.

Table 6 shows the performance comparison of the FSS-PSO model and historical operation. In Table 6, the values listed for each objective are explained as follows: sediment regulation – the sediment transport of the *TDG* station; ice/flood control – the discharge and water level of the *LJX* reservoir prior to flood seasons; hydropower generation – the hydropower generated by the *LYX* and *LJX* hydropower stations; and water supply – the water supply of the *LZ* section. The results demonstrate that the FSS-PSO model can satisfy all the objectives and obtain much better outcomes in all the objectives, as compared with historical operation, which indicate the FSS-PSO algorithm can be adequately applied to solving multi-objective optimization problems for producing suitable and satisfactory results.

4.3.5. Algorithm assessment

To assess the superiority and efficiency of the proposed FSS-PSO algorithm, the classical PSO and the CPSO are implemented with the same parameter setting of the FSS-PSO (Table 4). The results of the PSO, the CPOS and the FSS-PSO are listed in Table 7. The computer we use is Lenovo M6980 with 64-bit Windows 7 OS, Inter® Core™ 2 Duo CPU E7200 @2.53 GHz, 300GB RAM, and NVIDIA GeForce GT720 Graphics Card.

In Table 7, the hydropower generation amount of cascade hydropower stations obtained from the FSS-PSO is larger than those of the CPSO and the PSO by 0.65 billion kWh (4.8%) and 0.84 billion kWh (6.2%), respectively. Moreover, the scoured sediment amount obtained from the FSS-PSO achieves 38.51million tons, which is 12.6% and 22.5% more than those of the CPSO and the PSO, respectively. It is observed that under the same comparison conditions, the FSS-PSO produces better performances in all the four objectives than the CPSO and the PSO. Besides, the computations of the PSO and the CPSO take 18 s and 11 s, respectively, while the computation of the FSS-PSO takes only 5 s. That is to say, the FSS-PSO improves the efficiency of the PSO and the CPSO by 72% and 55%, respectively, which demonstrates the superiority of the FSS-PSO. We notice that the numbers of decision variables and constraints are not big because this study only deals with monthly operation in one year (2010); nevertheless, when dealing with daily operation in one year, the numbers of decision variables and constraints could be much bigger (more than 30 times), and thus the efficiency and effectiveness of the proposed FSS-PSO would become critical.

Fig. 10 shows the convergence curves of two objectives (hydropower generation, water and sediment regulation) for the PSO, the CPSO and the FSS-PSO. It can be observed that the convergence rates of the FSS-PSO in terms of both objectives are the fastest among the three algorithms, which demonstrates the FSS-PSO performs better than the CPSO and the PSO.

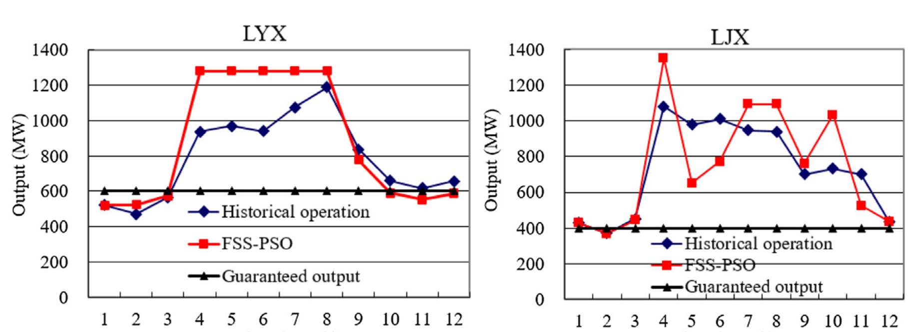

Fig. 8. Power generation output of LYX and LJX hydropower stations, respectively, for 2010.

Table 6
Performance comparison of the FSS-PSO model and historical operation.

Objective / Item	Obj.1 Sediment regulation (10^8t)	Obj.2 Ice control (m^3/s)/flood control (m)	Obj.3Hydropower generation (10^8 kWh)	Obj.4 Water supply ($10^8 m^3$)
Representative value[a]	0.5810	740, 490, 460, 380, 450 /1726	87.6	238.0
Historical operation[b]	0.1240	800, 491, 462, 391, 470 /1722	133.4	314.0
FSS-PSO model	0.6110	586, 490, 460, 380, 450 /1722	143.3	355.2

[a] Extremums of constraints: sediment regulation – the incoming sediment at the TDG station; ice/flood control – the maximum discharge and water level of the LJX prior to flood seasons (Table 3); hydropower generation – the minimum energy generated by the LYX and LJX hydropower stations (design capacity); and water supply – the minimum flow of the LZ section (Table 2).
[b] Historical data were extracted from Yellow River Sediment Bulletin (2010) and the Huanghe Hydropower Development Co., Ltd.

Table 7
Performance comparison among the PSO, the CPSO and the FSS-PSO.

	Hydropower generation (10^8 kWh)			Scoured sediment amount (10^8 tons)	Computation time(second)
	LYX	LJX	Cascade of LYX and LJX		
PSO	73.0	61.9	134.9	0.3144	18
CPSO	74.2	62.6	136.8	0.3420	11
FSS-PSO	77.7	65.6	143.3	0.3851	5

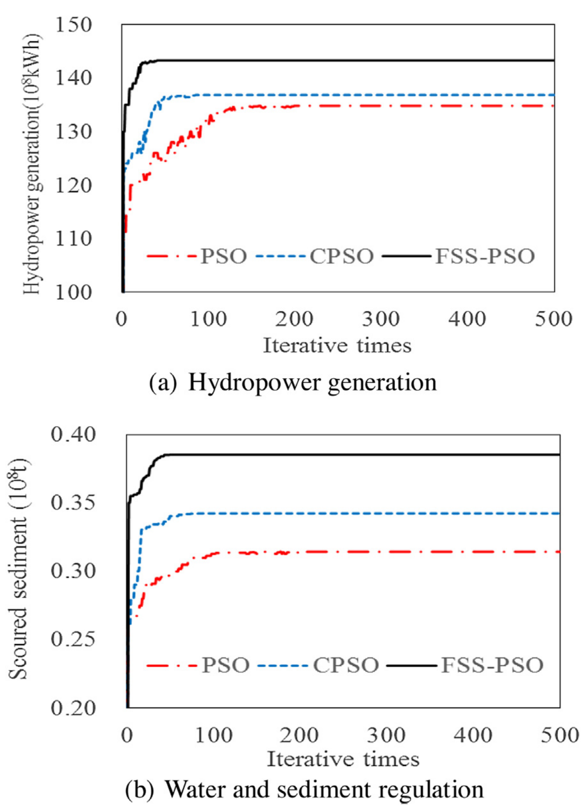

Fig. 10. Convergence curves of (a) hydropower generation and (b) water and sediment regulation obtained from the PSO, the CPSO and the FSS-PSO, respectively.

5. Conclusion

In this study, a multi-objective optimization model for the joint operation of two cascade reservoirs in the Upper Yellow River basin is proposed. We first design a dimensionality-reduction and constraint transformation procedure and then develop a novel and effective method that fuses a Feasible Search Space into the Particle Swarm Optimization algorithm, i.e. an improved FSS-PSO. We show that the proposed methodology is very effective in reducing the complexity of the system and efficient in identifying the feasible search space. The results demonstrate that the whole riverbed of the Ningxia-Inner Mongolia reaches could be well soured by artificial floods, which has important practical significance for improving the relationship between water and sediment, reducing the speed of sedimentation rate, and ensuring the safety of downstream reaches during flooding. Compared with historical operation, the result of the FSS-PSO model provides much better performance, e.g. producing 0.99 billion kWh more hydropower and providing 4.12 billion m^3 more water supply in the *LZ* section.

To demonstrate the efficiency of the FSS-PSO, the CPSO and the PSO are two comparative algorithms adopted in this study. Results indicate that as compared with the CPSO and the PSO, the FSS-PSO increases hydropower generation by 4.8% and 6.2% accordingly and increases the scoured sediment amount by 12.6% and 22.5% accordingly. Besides, the convergence rate of the FSS-PSO is the fastest and the computation time of the FSS-PSO improves 72% and 55%, respectively, as compared with the PSO and the CPSO. In sum, the superiority and efficiency of the proposed methodology is demonstrated through a complex multi-objective cascade reservoir operation system with two scenarios. While it is encouraging to find that the methodology could intelligently reduce the dimension of objectives and constraints and systematically condense the feasible search space through intelligibly eliminating redundant search space. We hope this work would lay a pathway for the systematical construction of multi-objective model and can be utilized to solve other complex engineering problems.

Acknowledgements

This study is supported by the National Department Public Benefit Research Foundation of Ministry of Water Resources, China (201501058); National Natural Science Foundation of China (51409210, 51190093) and Scientific Research Start Fund of Xi'an University of Technology. The data provided by the Huanghe Hydropower Development Co., Ltd and Yellow River Conservancy Commission, are great appreciated. Dr. Tao Bai serves as a post-doctoral fellow in National Taiwan University for the period of May–December in 2014, which is financially supported by the Ministry of Science and Technology (MOST), Taiwan (101-2923-B-002-001-MY3).

References

[1] M.H. Afshar, Large scale reservoir operation by constrained particle swarm optimization algorithms, J. Hydro-Environ. Res. 6 (1) (2012) 75–87, http://dx.doi.org/10.1016/j.jher.2011.04.003.

[2] M.S. Azadeh, A particle swarm algorithm for inspection optimization in serial multi-stage processes, Appl. Math. Model. 36 (4) (2012) 1455–1464, http://dx.doi.org/10.1016/j.apm.2011.09.037.
[3] T. Bai, J.X. Chang, F.J. Chang, Q. Huang, Y.M. Wang, G.S. Chen, Synergistic gains from the multi-objective optimal operation of cascade reservoirs in the Upper Yellow River basin, J. Hydrol. 523 (2015) 758–767, http://dx.doi.org/10.1016/j.jhydrol.2015.02.007.
[4] T. Bai, L. Wu, J.X. Chang, Q. Huang, Multi-objective optimal operation model of cascade reservoirs and its application on water and sediment regulation, Water Res. Manage. 29 (8) (2015) 2751–2770, http://dx.doi.org/10.1007/s11269-015-0968-0.
[5] A. Bhattacharya, P.K. Chattopadhyay, Solution of optimal reactive power flow using biogeography-based optimization, Int. J. Energy Power Eng. 3 (2010) 269–277.
[6] F.J. Chang, Y.T. Chang, Adaptive neuro-fuzzy inference system for prediction of water level in reservoir, Adv. Water Res. 29 (1) (2006) 1–10, http://dx.doi.org/10.1016/j.advwatres.2005.04.015.
[7] J.X. Chang, T. Bai, Q. Huang, D.W. Yang, Optimization of water resources utilization by PSO-GA, Water Res. Manage. 27 (10) (2013) 3525–3540, http://dx.doi.org/10.1007/s11269-013-0362-8.
[8] J.X. Chang, X.J. Meng, Z.Z. Wang, X.B. Wang, Q. Huang, Optimized cascade reservoir operation considering ice flood control and power generation, J. Hydrol. 519 (2014) 1042–1051, http://dx.doi.org/10.1016/j.jhydrol.2014.08.036.
[9] L.C. Chang, Guiding rational reservoir flood operation using penalty-type genetic algorithm, J. Hydrol. 354 (1–4) (2008) 65–74, http://dx.doi.org/10.1016/j.jhydrol.2008.02.021.
[10] L.C. Chang, F.J. Chang, Multi-objective evolutionary algorithm for operating parallel reservoir system, J. Hydrol. 377 (1–2) (2009) 12–20, http://dx.doi.org/10.1016/j.jhydrol.2009.07.061.
[11] L.C. Chang, F.J. Chang, K.W. Wang, S.Y. Dai, Constrained genetic algorithms for optimizing multi-use reservoir operation, J. Hydrol. 390 (1–2) (2010) 66–74, http://dx.doi.org/10.1016/j.jhydrol.2010.06.031.
[12] Y.H. Chen, F.J. Chang, Evolutionary artificial neural networks for hydrological systems forecasting, J. Hydrol. 367 (1–2) (2009) 125–137, http://dx.doi.org/10.1016/j.jhydrol.2009.01.009.
[13] Y.M. Chiang, F.J. Chang, Integrating hydrometeorological information for rainfall-runoff modelling by artificial neural networks, Hydrol. Process. 23 (11) (2009) 1650–1659, http://dx.doi.org/10.1002/hyp.7299.
[14] K. Deb, D. Saxena, Searching for Pareto-optimal solutions through dimensionality reduction for certain large-dimensional multi-objective optimization problems, Proceedings of the World Congress on Computational Intelligence (WCCI-2006) (2006) 3352–3360.
[15] Y.M. Feng, C.J. Li, M. Zhang, Research on the function of reservoir long-term operation based on improved particle swarm optimization (IPSO), Water Power. 34 (2) (2008) 94–97.
[16] P.J. Fleming, R.C. Purshouse, R.J. Lygoe, Many-objective Optimization: An Engineering Design Perspective Evolutionary Multi-criterion Optimization, Springer, Berlin, Heidelberg, 2005, pp. 14–32.
[17] X.Z. Gao, X. Wang, T. Jokinen, S.J. Ovaska, A. Arkkio, K. Zenger, A hybrid optimization method for wind generator design, Int. J. Innov. Comput. Inf. Control. 8 (6) (2012) 4347–4373.
[18] X.Z. Gao, X. Wang, S.J. Ovaska, Uni-modal and multi-modal optimization using modified harmony search methods, Int. J. Innov. Comput. Inf. Control. 5 (10) (2009) 2985–2996.
[19] S. Gaur, K.S. Raju, D.N. Kumar, D. Graillot, Multiobjective fuzzy optimization for sustainable groundwater management using particle swarm optimization and analytic element method, Hydrol. Process. 29 (19) (2015) 4175–4187, http://dx.doi.org/10.1002/hyp.10441.
[20] X. Guo, T. Hu, C. Wu, T. Zhang, Y. Lv, Multi-objective optimization of the proposed multi-reservoir operating policy using improved NSPSO, Water Res. Manage. 27 (7) (2013) 2137–2153, http://dx.doi.org/10.1007/s11269-013-0280-9.
[21] R. Hajiabadi, M. Zarghami, Multi-Objective reservoir operation with sediment flushing; case study of sefidrud reservoir, Water Resour. Manage. 28 (15) (2014) 5357–5376, http://dx.doi.org/10.1007/s11269-014-0806-9.
[22] W.C. Huang, L.C. Yuan, A drought early warning system on real-time multi-reservoir operations, Water Resour. Res. 40 (6) (2004) W06401, http://dx.doi.org/10.1029/2003WR002910.
[23] B. Kamali, S.J. Mousavi, K.C. Abbaspour, Automatic calibration of HEC-HMS using single-objective and multi-objective PSO algorithms, Hydrol. Process. 27 (26) (2013) 4028–4042, http://dx.doi.org/10.1002/hyp.9510.
[24] R.U. Kamodkar, D.G. Regulwar, Multipurpose reservoir operating policies: a fully fuzzy linear programming approach, J. Agric. Sci. Technol. 15 (6) (2013) 1261–1274 (WOS.000327139000016).
[25] J. Kennedy, R.C. Eberhart, Particle swarm optimization, in: IEEE International Conference on Neural Networks, IV, IEEE Service Center, Piscataway, NJ, 1995, pp. 1942–1948.
[26] N.M. Khan, T. Tingsanchali, Optimization and simulation of reservoir operation with sediment evacuation: a case study of the Tarbela Dam, Pakistan, Hydrol. Process. 23 (5) (2009) 730–747, http://dx.doi.org/10.1002/hyp.7173.
[27] D.X. Kong, C.Y. Miao, J.W. Wu, Q.Y. Duan, Q.H. Sun, A.Z. Ye, Z.H. Di, W. Gong, The hydro-environmental response on the lower Yellow River to the water–sediment regulation scheme, Ecol. Eng. 79 (2015) 69–79, http://dx.doi.org/10.1016/j.ecoleng.2015.03.009.
[28] F.F. Li, C.A. Shoemaker, J. Qiu, J.H. Wei, Hierarchical multi-reservoir optimization modeling for real-world complexity with application to the Three Gorges system, Environ. Modell. Softw. 69 (2015) 319–329, http://dx.doi.org/10.1016/j.envsoft.2014.11.030.
[29] G.Y. Li, Water and sediment regulation on the yellow river, in: International Yellow River Forum (IYRF), Zheng Zhou, China, 2009, pp. 25–29.
[30] Q. Li, Y.M. Wang, T. Bai, Review on water and sediment regulation of the Yellow River, J. Northwest A&F Univ. (Nat. Sci. Ed.) 42 (12) (2014) 1–7.
[31] R.H. Liang, J.C. Wang, Y.T. Chen, W.T. Tseng, An enhanced firefly algorithm to multiobjective optimal active/reactive power dispatch with uncertainties consideration, Int. J. Electr. Power Energy Syst. 64 (2015) 1088–1097.
[32] J.G. Luo, Y.T. Qi, J.C. Xie, X. Zhang, A hybrid multi-objective PSO-EDA algorithm for reservoir flood control operation, Appl. Soft Comput. 34 (2015) 526–538, http://dx.doi.org/10.1016/j.asoc.2015.05.036.
[33] R.T. Marler, J.S. Arora, Survey of multi-objective optimization methods for engineering, Struct. Multidiscip. O. 26 (6) (2004) 369–395.
[34] K. Massimiliano, A multi-start opposition-based particle swarm optimization algorithm with adaptive velocity for bound constrained global optimization, J. Glob. Optim. 55 (1) (2013) 165–188, http://dx.doi.org/10.1007/s10898-012-9913-4.
[35] S.J. Mousavi, M. Karamouz, M.B. Menhadj, Fuzzy-state stochastic dynamic programming for reservoir operation, J. Water Res. Plan. Manage. 130 (6) (2004) 460–470, http://dx.doi.org/10.1061/(ASCE)0733-9496(2004)130:6(460).
[36] H.A. Taboada, F. Baheranwala, D.W. Coit, N. Wattanapongsakorn, Practical solutions for multi-objective optimization: an application to system reliability design problems, Reliab. Eng. Syst. Safe. 92 (3) (2007) 314–322.
[37] K.W. Wang, L.C. Chang, F.J. Chang, Multi-tier interactive genetic algorithms for the optimization of long-term reservoir operation, Adv. Water Res. 34 (10) (2011) 1343–1351, http://dx.doi.org/10.1016/j.advwatres.2011.07.004.
[38] Y. Wang, J.Z. Zhou, C. Zhou, Y.Q. Wang, H. Qin, Y.L. Lu, An improved self-adaptive PSO technique for short-term hydrothermal scheduling, Expert Syst. Appl. 39 (3) (2012) 2288–2295, http://dx.doi.org/10.1016/j.eswa.2011.08.007.
[39] B. Xiang, C.M. Ji, Q.S. Luo, Immune particle swarm optimization algorithm and its application in reservoir operation optimization, J. Hohai Univ. (Nat. Sci.) 36 (2) (2008) 198–202.
[40] X.A. Yin, Z.F. Yang, W. Yang, Y.W. Zhao, H. Chen, Optimized reservoir operation to balance human and riverine ecosystem needs: model development, and a case study for the Tanghe reservoir, Tang river basin, China, Hydrol. Process. 24 (4) (2010) 461–471, http://dx.doi.org/10.1002/hyp.7498.
[41] X.B. Yu, J. Cao, H.Y. Shan, L. Zhu, J. Guo, An adaptive hybrid algorithm based on particle swarm optimization and differential evolution for global optimization, Sci. World J. (2014) 25–40, http://dx.doi.org/10.1155/2014/215472.
[42] S.H. Zhang, Q. Huang, H.S. Wu, J.X. Yang, A modified particle swarm optimizer for optimal operation of hydropower station, J. Hydroelectr. Eng. 26 (1) (2007) 1–5.
[43] X.H. Zhang, Y.S. Zheng, H.X. Shang, Research on scouring and deposition law and characteristics of sediment transport of Ningxia-Inner Mongolia reaches, Yellow River 30 (11) (2008) 42–44.
[44] X.S. Zhang, R. Srinivasan, M. Van Liew, On the use of multi-algorithm, genetically adaptive multi-objective method for multi-site calibration of the SWAT model, Hydrol. Process. 24 (8) (2010) 955–969, http://dx.doi.org/10.1002/hyp.7528.
[45] Z.B. Zhang, Y.Z. Jiang, S.H. Zhang, S.M. Geng, H. Wang, G.Q. Sang, An adaptive particle swarm optimization algorithm for reservoir operation optimization, Appl. Soft Comput. 18 (2014) 167–177, http://dx.doi.org/10.1016/j.asoc.2014.01.034.